

# Supercontinuum Generation in the Low-Peak-Power Regime Using a Single-Stage Multipass Cell

ZEYANG HU<sup>\*</sup>, KILIAN FRITSCH, AND OLEG PRONIN

n2-Photonics GmbH, Hans-Henny-Jahnn-Weg 53, 22085 Hamburg, Germany

*\*zeyang.hu@n2-photonics.de*

Received XX Month XXXX; revised XX Month, XXXX; accepted XX Month XXXX; posted XX Month XXXX (Doc. ID XXXXX); published XX Month XXXX

We demonstrate a single-stage multipass cell (MPC) compressor driven directly by a 500 nJ, 5 W, 120 fs, 10 MHz oscillator that delivers efficient spectral broadening from 800 to 1200 nm with >75% transmission. The compressed pulses approach the Fourier limit (FTL) of 8.1 fs, representing, to the best of our knowledge, the first realization of supercontinuum (SC) generation and compression in a single-stage MPC at such low, MW-level, input peak power. This compact, high-repetition-rate source holds strong potential for multiphoton microscopy and coherent Raman imaging.

Pulse compression and spectral broadening have become essential methods in a wide range of scientific and technological fields [1]. Besides their role in basic research, these techniques are now widely used in applied and industrial scenarios, including microscopy [2–5] and spectroscopy [6–8], where high sensitivity and stability are often required. These techniques generate ultrashort pulses with broadened spectra, improving detection sensitivity and advancing high-resolution optical measurements.

Large mode area (LMA) photonic crystal fibers (PCFs) sources are an established method for SC generation. SC generation in LMA fibers is primarily driven by self-phase modulation (SPM) and optical wave breaking (OWB). Increasing the mode area reduces optical intensity and nonlinear effects, thereby helping suppress self-focusing and heat accumulation and enabling higher-power operation without exceeding the material damage threshold [9]. Südmeyer et al. [10] first extended spectral broadening to high average power (18 W) by employing LMA PCFs, generating 33-fs pulses. However, enlarging the mode area, while allowing higher power transmission, limits spectral broadening, highlighting the trade-off between fiber damage and nonlinear performance [11]. In 2018, LMA-12 PCFs (NKT Photonics) were tested in [12]. This fiber had a mode field diameter (MFD) of 10.3  $\mu\text{m}$  at 1064 nm and a length of

8–10 cm. It generated spectra from 800 nm to 1200 nm when pumped by a Yb:YAG thin-disk oscillator with a peak power of 4.6 MW. However, surface damage was observed on the LMA-12 fibers even at input powers below the damage threshold. In the same year, Shen et al. [13] investigated LMA-15 PCFs with a core diameter of 15.1  $\mu\text{m}$  and an MFD of 12.8  $\mu\text{m}$  at 1064 nm. A 5-m-long fiber was pumped by a picosecond Nd:YVO<sub>4</sub> laser (1064 nm, 7 ps, 1 MHz) with 3.8 W pump powers, corresponding to a peak power of approximately 0.54 MW. The fiber produced a broad spectrum extending from 600 nm to 1600 nm. However, the authors reported that 3.8 W pump power was already close to the damage threshold of the LMA-15 fiber, mainly due to loss and heating near the bend edge. Although these fibers are effective for spectral broadening, their micrometer-scale core size requires precise alignment to ensure efficient coupling of the pump laser into the fiber: Seidel et al. [12] reported coupling efficiencies of 65–80% for the tested fibers; thus, the LMA-12 fiber can be reasonably expected to exhibit a coupling efficiency of approximately 70–75%; LMA-15 tested by Shen et al. [13] only had coupling efficiency at around 60%. Both Ref. [12] and Ref. [13] required specific optical setups (e.g., focusing lenses) to mode match the beam in order to allow efficient coupling into the fiber. In practical situations, the coupling condition is highly sensitive to external perturbations, and even slight drifts in the pump laser beam induced by vibrations, thermal fluctuations, or mechanical instability can lead to a noticeable degradation of coupling efficiency [14]. Such variations not only induce unwanted intensity fluctuations at the fiber input but also accumulate during propagation, leading to an increase in the relative intensity noise (RIN) of the generated supercontinuum [15]. Guandalini et al. employed filamentation in noble gases to avoid coupling

issues, achieving 26% overall transmission limited by beam aperturing before the second stage [16].

The Herriott-type MPC-based spectral broadening approach stands for its simplicity and scalability [17], requiring only two curved mirrors and a Kerr medium. More importantly, MPC can tolerate small mode mismatches [18] without inducing additional transmission losses or optical damage, thereby enhancing system robustness and reducing daily maintenance requirements. In MPC-based spectral broadening, SPM is enhanced by increasing the effective nonlinear interaction length through multiple beam passes within the nonlinear medium. Nevertheless, reports of pulse compression to sub-10 fs durations are still few [19-23]. This results from the challenge of maintaining the required group delay dispersion (GDD) bandwidth [24] and controlling the dispersion introduced by the mirrors, which in turn reduces the effectiveness of the spectral broadening. Moreover, losses introduced by dielectric mirrors and the propagation medium (especially solid media [23]) in such designs are also non-negligible.

In this work, we investigate the MW-level peak power range for SC in MPC. The main motivation is to apply MPC broadening to low peak power laser systems, especially oscillators (e.g. FLINT, Light Conversion). With only 500 nJ input energy (5 MW peak power at 10 MHz), the system generated broadband output spanning 800–1200 nm with over 75% transmission efficiency. The FTL pulse corresponding to the measured spectrum has a full width at half maximum (FWHM) duration of approximately 8.1 fs, demonstrating the capability of this compact, low-energy MPC scheme to deliver high-quality ultrashort pulses. Compared with earlier MPC systems (Table 1), our system shows that efficient few-cycle generation is possible without extreme peak powers.

Table 1. Overview of MPC systems with sub-10 fs pulse durations<sup>1</sup>

Units	This paper	[19]	[20]	[21]	[22]	[23]
$P_{pk, input}$	MW	<b>5</b>	48	$5.0 \times 10^3$	$8.0 \times 10^3$	$1.7 \times 10^3$
$P_{pk, output}$	MW	<b>3.75</b>	$1.0 \times 10^3$	$6.0 \times 10^4$	$3.0 \times 10^5$	$3.0 \times 10^4$
$\tau_{input}$	fs	<b>120</b>	230	200	$1.2 \times 10^3$	$1.2 \times 10^3$
$\tau_{output}$	fs	<b>8.1</b>	7	6.9	9.6	13
$P_{avg, input}$	W	<b>5</b>	12	500	9.45	$200^2$
$P_{avg, output}$	W	<b>3.75</b>	<b>10</b>	388	6.7	$37^2$
Transm.	%	<b>75</b>	84	78	70	$37^3$
$f_{rep.}$	MHz	<b>10</b>	1	0.5	0.001	0.1
Medium	-	FS <sup>4</sup>	Ar, FS	Ar, He	Ar, Ne	Kr
						FS

<sup>1</sup>Peak power,  $P_{pk}$ ; pulse durations,  $\tau$ ; average powers,  $P_{avg}$ ; overall transmission calculated as system input/system output,  $Transm.$ ; repetition

rate,  $f_{rep.}$ . <sup>2</sup>In-burst average power. <sup>3</sup>Calculated from two MPC stages only; power was reduced before the second stage to prevent damage. <sup>4</sup>FS: Fused Silica.

The experimental setup is illustrated in Fig. 1. A commercial oscillator (FLINT, Light Conversion) served as the driving source, delivering 120 fs pulses at a repetition rate of 10 MHz with 0.5  $\mu$ J pulse energy, corresponding to an average power of 5 W. The laser output was adjusted to provide a peak power suitable for driving the setup, which was designed to achieve a spectral bandwidth of 800–1200 nm. The laser output was mode-matched to the MPC's eigenmode using a telescope. The Herriott cell consisted of two highly reflective mirrors with a radius of curvature of 50 mm (both have  $-50$  fs<sup>2</sup> of GDD), separated by 97 mm. In this configuration, the beam reflected 68 passes within the MPC, and a 2 mm-thick AR-coated fused silica was placed at the center of the MPC. A thicker fused silica plate was avoided because it would introduce additional positive dispersion, leading to temporal pulse broadening and a reduction in peak power, thereby degrading the nonlinear spectral broadening. After 68 passes through the fused silica plate, the accumulated B-integral reached 27.3 rad (0.4 rad per pass). The MPC was operated in ambient air, where the total B-integral contribution from air was negligible, approximately  $4 \times 10^{-3}$  rad. The system maintained 75% transmission, primarily limited by losses in the AR-coated fused silica and the dispersive mirrors [25]. Pulse durations of  $\sim$ 10 fs were achieved through five dispersive-mirror reflections, each introducing  $-150$  fs<sup>3</sup> of TOD, and a 22 cm CaF<sub>2</sub> plate for GDD compensation.

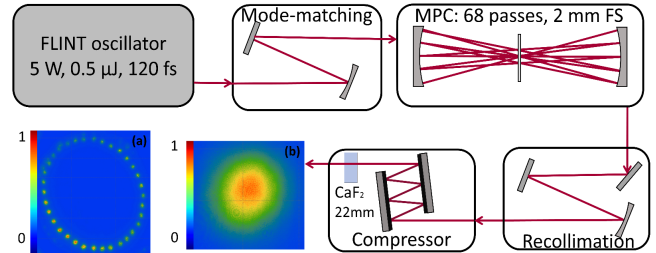


Fig. 1. Schematic of the nonlinear broadening and pulse compression (FS: Fused Silica) (a) One of the MPC patterns on a CCD camera. (b) Output beam profile after MPC stage.

Fig. 2 shows the spectra obtained in our system. The output spectrum after MPC (red) is significantly broadened, extending from 800 nm to 1200 nm. The logarithmic representation (dashed lines) further emphasizes the efficient generation of weak spectral components at the spectral edges, which are less visible on the linear scale (the spectrometer exhibits a noise floor at around  $10^{-3}$  on the log scale). The temporal profile retrieved from the linear spectrum is shown in Fig. 3. The FTL pulse has a FWHM of approximately 8.1 fs, confirming that the generated spectrum is sufficient to support sub-10 fs pulses once residual dispersion is fully compensated.

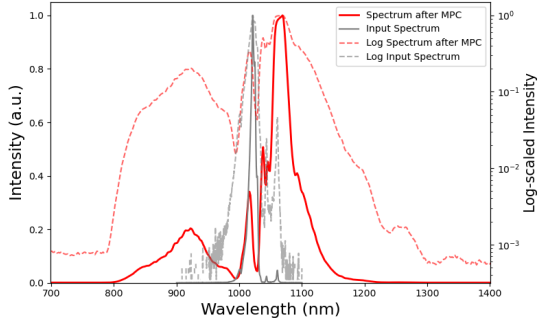


Fig. 2. Spectral characteristics of the MPC output.

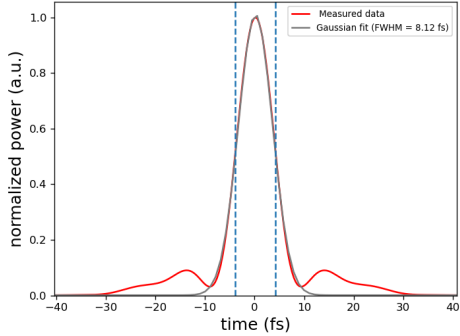


Fig. 3. FTL temporal profile retrieved from the output spectrum (Fig. 2): pulse duration of 8.1 fs compared with a Gaussian fit.

Fig. 1(b) shows the measured output beam profile after the MPC stage. Elliptical fitting of the beam indicates diameters of approximately 4.2 mm ( $D_x$ ) and 4.0 mm ( $D_y$ ) along the axes, with an ellipticity of 0.94, confirming that the output beam remains nearly circular with no visible signs of distortion. The beam quality was further measured to be  $M_{eff}^2 = 1.107 \pm 0.014$  (ISO11146-2), indicating that the output beam is close to an ideal Gaussian profile (Fig. 4). It should be noted that, due to the 1100 nm upper sensitivity limit of the Si sensor, the beam quality was verified only within this spectral range.

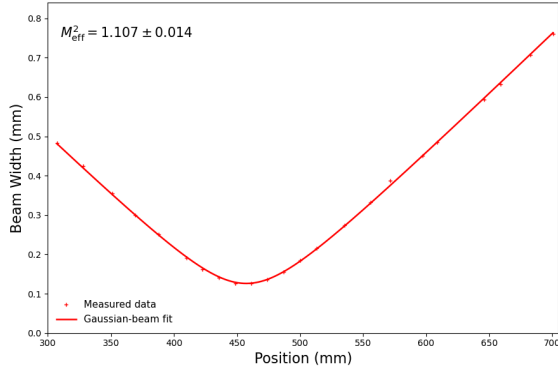


Fig. 4. Measurement of beam quality of  $M^2$ . The central wavelength of 1030 nm is chosen for the measurement.

Unfortunately, the FLINT oscillator was available only for a limited period, which prevented the completion of the compression experiments. Instead, a comparable setup was implemented using a regenerative amplifier system attenuated to deliver 0.4 W average power (0.4  $\mu$ J, 1 MHz, 90 fs) from a Pharos UP laser (Light Conversion). The main goal was to verify the feasibility of the compression. The setup used the same MPC mirrors, but separated by 98 mm, a 2 mm-thick AR-coated fused silica plate was positioned 4 mm from the MPC center. After 58 passes through the fused silica plate, the accumulated B-integral reached 20.4 rad (0.4 rad per pass). Pulse characterization was done with a D-max device (Sphere Ultrafast Photonics). The comparison between the measured and simulated spectra is presented in Fig. 5. In our simulation, an input power of 0.37 W (0.37  $\mu$ J, 1 MHz, 100 fs) was used, incorporating an average mirror reflection loss of 0.3% per bounce and a medium transmission loss of 0.2% to account for experimental conditions. The slightly reduced input power accounts for propagation losses. The result shows a good agreement between the simulated and experimental spectra.

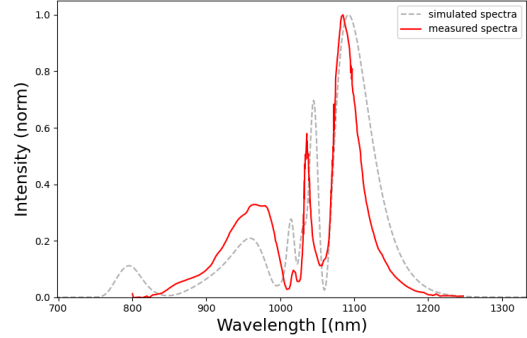


Fig. 5. Comparison between simulated and measured spectra.

Fig. 6 shows D-scan retrieval results in the spectral domain. In Fig. 6(a), the D-scan retrieval taken after the MPC indicates a distorted phase with  $-3 \times 10^2$  fs<sup>2</sup> of GDD and  $+1.8 \times 10^3$  fs<sup>3</sup> of TOD, indicating the pulse accumulated strong dispersion during the MPC propagation. A numerical simulation of the compressor was available in the D-scan software (Fig. 6(b)), indicating that a compressed pulse could be achieved using CaF<sub>2</sub> and chirped mirrors. Fig. 6(c) shows the experimentally retrieved result after the actual compressor, which was in good agreement with the simulated result, confirming successful dispersion compensation. The pulse duration was reduced to around 10 fs with a relative peak power compared to FTL is 78.5% (Fig. 6(d), the retrieval with a root-mean-square error of 0.6%), very close to the results shown in Fig. 3. The presence of the pedestal suggests incomplete dispersion compensation, which will be further optimized in future work.

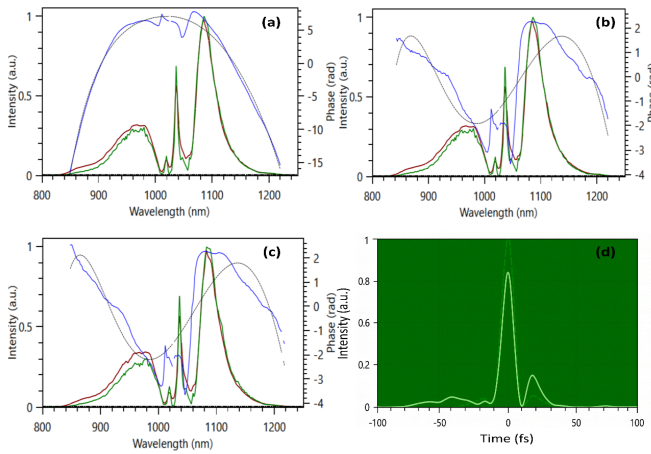


Fig. 6. (a)-(c) D-scan retrieval results in the spectral domain. Red line: Measured linear spectrum. Green line: Retrieved linear spectrum. Blue line: Retrieved spectral phase. Black line: 4th order polynomial fit of the spectral phase. (a) After the MPC output (before the compressor). (b) After the MPC with the simulated compressor in D-scan software. (c) After the actual compressor (CaF<sub>2</sub> + chirped mirrors). (d) Temporal intensity compared to FTL of the spectrum in Fig. 6 (c). Dashed green: Temporal intensity profile of the transform-limited pulse-10.32 fs. Light Green: Temporal intensity profile of the measured pulse-10.0 fs). Relative peak power: 78.5%.

We demonstrated an efficient single-stage MPC compressor directly driven by an oscillator. Operating at only 500 nJ (5 MW peak power, 10 MHz repetition rate), the system achieved spectral broadening from 800 to 1200 nm with 75% transmission. Subsequent compression yielded pulses approaching the FTL of 8.1 fs. Compared with previously reported MPC systems, our setup operates at 10 times lower peak powers while still delivering few-cycle pulses with high beam quality. This highlights that efficient sub-10 fs pulse generation can be realized without extreme GW-level peak powers, thus offering a practical alternative to LMA fibers. Simulations indicate that similar broadening can be achieved with only 4 MW peak power. Due to its compact footprint, and excellent output characteristics, the setup holds strong potential for demanding applications in nonlinear microscopy, as well as in other areas where ultrashort, high-repetition-rate light sources are required.

**Acknowledgement.** We would like to thank the Light Conversion team, namely Valdas Maslinskas and Mantvydas Mikulis, for providing the lasers that enabled these remarkable measurements. We also thank Igor Rebrov and Tomin Joy for valuable discussions, and Christian Franke for designing the optomechanical components.

**Disclosures.** The authors declare a conflict of interest. The work was funded by n2-Photonics GmbH, which commercializes the

pulse-shortening technology. The company was co-founded by Oleg Pronin and Kilian Fritsch.

**Data availability.** Data underlying the results presented in this paper are not publicly available at this time but may be obtained from the authors upon reasonable request.

## References

1. G. Mourou, *Rev. Mod. Phys.* **91**, 030501 (2019).
2. Y. Liu, H. Tu, W. A. Benalcazar, et al., *IEEE J. Sel. Top. Quantum Electron.* **18**, 1209 (2012).
3. H. Tu and S. A. Boppart, *Laser Photon. Rev.* **7**, 628 (2013).
4. V. T. Hoang, Y. Boussafa, L. Sader, et al., *Front. Photon.* **3**, 940902 (2022).
5. G. Wang, J. Shi, R. R. Iyer, et al., *Adv. Photon. Nexus*, **3**, 046012 (2024).
6. A. Pashkin, A. Sell, T. Kampfrath, et al., *New J. Phys.* **15**, 065003 (2013).
7. Y. Zhang, S. Ciao, L. Sun, et al., *Opt. Laser Technol.* **170**, 110288 (2024).
8. I. Zorin, P. Gattinger, A. Ebner, et al., *Opt. Express*, **30**, 5222 (2022).
9. M. D. Nielsen, Ph.D. dissertation, *Technical University of Denmark*, (2004).
10. T. Südmeyer, F. Brunner, E. Innerhofer, et al., *Opt. Lett.* **28**, 1951 (2003).
11. J. Fekete, P. Rácz, and P. Dombi, *Appl. Phys. B* **111**, 415 (2013).
12. M. Seidel, X. Xiao, and A. Hartung, *IEEE J. Sel. Top. Quantum Electron.* **24**, 1 (2018).
13. Y. Shen, A. A. Voronin, A. M. Zheltikov, et al., *Sci. Rep.* **8**, 9526 (2018).
14. A. M. Heidt, D.-M. Spangenberg, A. Rampur, et al., *The Supercontinuum Laser Source*, R. R. Alfano, Ed., pp. 299–341 (2022).
15. C. R. Smith, R. D. Engelsholm, and O. Bang, *Opt. Express*, **30**, 8136 (2022).
16. A. Guandalini, P. Eckle, M. Anscombe, et al., *J. Phys. B At. Mol. Opt. Phys.* **39**, S257 (2006).
17. J. Schulte, T. Sartorius, J. Weitenberg, et al., *Opt. Lett.* **41**, 4511 (2016).
18. A. Vernaleken, P. Rußbüldt, T. Sartorius, et al., German Patent DE 10 2014 007 159 B4, Apr. 13 (2017).
19. S. Goncharov, K. Fritsch, and O. Pronin, *Opt. Lett.* **48**, 147 (2023).
20. M. Müller, J. Buldt, H. Stark, et al., *Opt. Lett.* **46**, 2678 (2021).
21. S. Rajhans, E. Escoto, N. Khodakovskiy, et al., *Opt. Lett.* **48**, 4753 (2023).
22. P. Balla, A. Bin Wahid, I. Sytcevich, et al., *arXiv:2003.11070* (2020).
23. A.-L. Viotti, C. Li, G. Arisholm, et al., *Opt. Lett.* **48**, 984 (2023).
24. I. Gražulevičiūtė, M. Skeivytė, E. Keblytė, et al., *Lith. J. Phys.* **55**, (2015).
25. V. Pervak, I. Ahmad, M. K. Trubetskov, et al., *Opt. Express*, **17**, 7943 (2009).